Visual Metrology with Uncalibrated Radial Distorted Images

Xiaoming Deng [1,2], Fuchao Wu [2], Yihong Wu [2], Fuqing Duan[3,2]
[1] *Virtual Reality Laboratory, Institute of Computing Technology, Chinese Academy of Sciences, Beijing, P. R. China*
[2] *National Laboratory of Pattern Recognition(NLPR), Institute of Automation, Chinese Academy of Sciences, Beijing, P. R. China*
[3] *College of Information Science and Technology, Beijing Normal University,*
E-mails: idengxm@gmail.com, {fcwu,yhwu,fqduan}@nlpr.ia.ac.cn

Abstract

Visual metrology methods with radial distorted images usually require a radial distortion model and a pre-calibration. In this paper, we propose a novel 3D metrology algorithm with at least three uncalibrated radial distorted images, and also derive a 2D metrology algorithm with at least two uncalibrated radial distorted images. The algorithm does not require a radial distortion model or calibrating camera intrinsic parameters except for radial distortion center, which can be usually known as a prior or computed easily, and correspondences of control points with known coordinates. The algorithm is of high accuracy, and robust to noise due to no requirement for specific radial distortion models. Experimental results show the feasibility and accuracy of the algorithm.

1. Introduction

Visual metrology has been used in applications such as traffic accident investigation, and architecture measurement [3, 4, 5]. The visual metrology algorithms in the literature can be broadly divided into two categories. The classical algorithm is to reconstruct the metric structure of the scene by stereo-vision techniques [7]. If the Euclidean reconstruction of a scene is obtained, then geometrical information such as distance and angle can be recovered. However, accurate Euclidean reconstruction is not easy since errors introduced by camera calibration may propagate along the computational process and cause a loss of accuracy to the final results. The other one is to use a single uncalibrated image [3, 4, 8]. In [4], a homography based approach to distance measurement on a plane was proposed, where the homography was computed from four specified control points on the plane. The same problem was also discussed in [8], where several other approaches to recovering the homography and taking measurement on a space plane were proposed.

The above algorithms are designed for perspective cameras, and can only do visual metrology within a fairly small view field. Omnidirectional cameras with radial distortion have a large view field [2], and the above metrology algorithms can not be used for these cameras due to distortion. If cameras with radial distortions are calibrated, visual metrology is straightforward. However, for most omnidirectional cameras except central catadioptric cameras, the accurate radial distortion models are not available [1], so the metrology results will greatly rely on the assumed distortion model. Up to now, few attempts have been focused on visual metrology with uncalibrated radial distorted images.

In this paper, we propose a novel 3D metrology algorithm with at least three uncalibrated radial distorted images, and also derive a 2D metrology algorithm with at least two uncalibrated radial distorted images. The main contribution is that the proposed metrology algorithm with radial distorted images does not need specific radial distortion models or calibration. In addition, the algorithm does not suppose the used images are captured with the same cameras. The radial distortion center is the only intrinsic parameter we need, and it can be set as the center of mirror contour image or the image center with the development of camera manufacturing technique[10]. Alternatively, the radial distortion center can be calibrated easily with the geometric invariants [9]. The detail of the proposed algorithm will be given in the main text. Simulating as well as real experiments are given to illustrate the feasibility and effectiveness.

2. Main Idea of This Algorithm

Geometric distortion of a camera lens can be typically classified into two classes, radial and tangential. Central catadioptric cameras and some off-the-

978-1-4244-2175-6/08/$25.00 ©2008 IEEE

shelf wide angle cameras have only radial distortion [1] [9, 10]. Radial distortion is a nonlinear transformation of a pixel along the direction from the image center to the pixel.

The radial distortion center of a camera can be computed with geometric invariants or center of mirror contour image as in [9, 10]. After the radial distortion center of a camera is obtained, we move the image coordinate system to the radial distortion center.

In this work, an image point is denoted by $\mathbf{m} = (u, v, 1)^T$ in the homogenous coordinates, and a radial distortion model is denoted by $L(u, v)$. Then the rectified image point of $\mathbf{m} = (u, v, 1)^T$ with $L(u, v)$ can be computed by the following equation [6]:

$$\hat{\mathbf{m}}_u = (u, v, L(u, v))^T \tag{1}$$

Hereafter, we call the plane that contains the rectified image points as a rectified image plane.

If $\mathbf{m}$ is the image of a 3D point $\mathbf{X} = (x, y, z)^T$, then the mapping between $\hat{\mathbf{m}}_u$ and $\hat{\mathbf{X}} = (x, y, z, 1)^T$ is a projective transformation, and can be expressed by:

$$\hat{\mathbf{m}}_u \approx \mathbf{P}\hat{\mathbf{X}}, \hat{\mathbf{m}}_u \times \mathbf{P}\hat{\mathbf{X}} = 0 \tag{2}$$

Usually, $\mathbf{P}$ is called the projective matrix between the space point and the rectified image plane, and it is a 3×4 homogeneous matrix with 11 degrees of freedom as it can only be determined up to a scale factor.

Let $\mathbf{P} \triangleq \begin{pmatrix} \mathbf{p}_1^T \\ \mathbf{p}_2^T \\ \mathbf{p}_3^T \end{pmatrix} = \begin{pmatrix} p_{11} & p_{12} & p_{13} & p_{14} \\ p_{21} & p_{22} & p_{23} & p_{24} \\ p_{31} & p_{32} & p_{33} & p_{34} \end{pmatrix}$

Then the equation (2) can be rewritten as:

$$\begin{cases} v\mathbf{p}_3^T\hat{\mathbf{X}} - L(u, v)\mathbf{p}_2^T\hat{\mathbf{X}} = 0 \\ L(u, v)\mathbf{p}_1^T\hat{\mathbf{X}} - u\mathbf{p}_3^T\hat{\mathbf{X}} = 0 \\ u\mathbf{p}_2^T\hat{\mathbf{X}} - v\mathbf{p}_1^T\hat{\mathbf{X}} = 0 \end{cases} \tag{3}$$

The 3rd equation in (3) is irrelevant to the distortion model $L(u, v)$. We can establish a set of homogeneous linear equations in $\mathbf{p}_1$ and $\mathbf{p}_2$ by the 3rd equation in (3). Since there are only 8 variables in $\mathbf{p}_1$ and $\mathbf{p}_2$, we can determine $(\mathbf{p}_1, \mathbf{p}_2)$ up to a scale factor with at least 7 correspondences of known 3D points and their images by solving a set of linear equations. After the vectors $(\mathbf{p}_1, \mathbf{p}_2)$ are computed, 3D visual metrology from at least three uncalibrated images is possible. If the images of a point $\widehat{\mathbf{X}} = (\widehat{x}, \widehat{y}, \widehat{z}, 1)^T$ under three views are $\widehat{\mathbf{m}} = (\widehat{u}, \widehat{v}, 1)^T$, $\widehat{\mathbf{m}'} = (\widehat{u'}, \widehat{v'}, 1)^T$ and $\widehat{\mathbf{m}''} = (\widehat{u''}, \widehat{v''}, 1)^T$, then we obtain three linear equations in $(\widehat{x}, \widehat{y}, \widehat{z})$ by the 3rd equation in (3):

$$\mathbf{A}_1 \begin{pmatrix} \widehat{x} \\ \widehat{y} \\ \widehat{z} \end{pmatrix} = \mathbf{b}_1 \tag{4}$$

where

$$\mathbf{A}_1 \triangleq \begin{pmatrix} \widehat{u}p_{21} - \widehat{v}p_{11} & \widehat{u}p_{22} - \widehat{v}p_{12} & \widehat{u}p_{23} - \widehat{v}p_{13} \\ \widehat{u'}p'_{21} - \widehat{v'}p'_{11} & \widehat{u'}p'_{22} - \widehat{v'}p'_{12} & \widehat{u'}p'_{23} - \widehat{v'}p'_{13} \\ \widehat{u''}p''_{21} - \widehat{v''}p''_{11} & \widehat{u''}p''_{22} - \widehat{v''}p''_{12} & \widehat{u''}p''_{23} - \widehat{v''}p''_{13} \end{pmatrix}$$

$$\mathbf{b}_1 \triangleq \begin{pmatrix} \widehat{v}p_{14} - \widehat{u}p_{24} \\ \widehat{v'}p'_{14} - \widehat{u'}p'_{24} \\ \widehat{v''}p''_{14} - \widehat{u''}p''_{24} \end{pmatrix}$$

And then the point $\widehat{\mathbf{X}} = (\widehat{x}, \widehat{y}, \widehat{z}, 1)^T$ can be determined linearly with (4).

If $\mathbf{X}$ is on a space plane, assuming the space plane is at $z = 0$ without loss of generality, then the relationship between $\hat{\mathbf{m}}_u$ and $\hat{\mathbf{X}}$ can be expressed by:

$$\begin{aligned} \hat{\mathbf{m}}_u &\approx \mathbf{P}\hat{\mathbf{X}} \\ &= \begin{pmatrix} p_{11} & p_{12} & p_{13} & p_{14} \\ p_{21} & p_{22} & p_{23} & p_{24} \\ p_{31} & p_{32} & p_{33} & p_{34} \end{pmatrix} \begin{pmatrix} x \\ y \\ 0 \\ 1 \end{pmatrix} \\ &= \underbrace{\begin{pmatrix} p_{11} & p_{12} & p_{14} \\ p_{21} & p_{22} & p_{24} \\ p_{31} & p_{32} & p_{34} \end{pmatrix}}_{\mathbf{H}} \underbrace{\begin{pmatrix} x \\ y \\ 1 \end{pmatrix}}_{\tilde{\mathbf{X}}} = \mathbf{H}\tilde{\mathbf{X}} \end{aligned} \tag{5}$$

where $\tilde{\mathbf{X}}$ is denoted as $\tilde{\mathbf{X}} = (x, y, 1)^T$.

Usually, $\mathbf{H}$ is called the homography between the space plane and the rectified image plane, and it is a 3×3 non-singular homogeneous matrix with 8 degrees of freedom and can be determined up to a scale factor.

Denote $\mathbf{H} \triangleq \begin{pmatrix} \mathbf{h}_1^T \\ \mathbf{h}_2^T \\ \mathbf{h}_3^T \end{pmatrix} = \begin{pmatrix} p_{11} & p_{12} & p_{14} \\ p_{21} & p_{22} & p_{24} \\ p_{31} & p_{32} & p_{34} \end{pmatrix}$.

Then the equation (5) can be rewritten as:

$$\begin{cases} v\mathbf{h}_3^T\tilde{\mathbf{X}} - L(u, v)\mathbf{h}_2^T\tilde{\mathbf{X}} = 0 \\ L(u, v)\mathbf{h}_1^T\tilde{\mathbf{X}} - u\mathbf{h}_3^T\tilde{\mathbf{X}} = 0 \\ u\mathbf{h}_2^T\tilde{\mathbf{X}} - v\mathbf{h}_1^T\tilde{\mathbf{X}} = 0 \end{cases} \tag{6}$$

The 3rd equation in (6) is irrelevant to the distortion model $L(u, v)$. We can establish a set of homogeneous linear equations in $\mathbf{h}_1$ and $\mathbf{h}_2$ by the 3rd equation in (6). Since there are only 6 variables in $\mathbf{h}_1$ and $\mathbf{h}_2$, we can determine $(\mathbf{h}_1, \mathbf{h}_2)$ up to a scale factor with at least 5 correspondences of known planar points and their images by solving a set of linear equations.

[1] It should be noted that our method does not assume that the used camera has a single viewpoint. The method can be applied in visual metrology of wide angle images with only radial distortion.

After the vectors $(\mathbf{h}_1, \mathbf{h}_2)$ are computed, visual metrology on the plane determined by the above coplanar points is possible with at least two uncalibrated images. If the images of a point $\breve{\mathbf{X}} = (\breve{x}, \breve{y}, 1)^T$ under two views are $\breve{\mathbf{m}} = (\breve{u}, \breve{v}, 1)^T$, $\breve{\mathbf{m}}' = (\breve{u'}, \breve{v'}, 1)^T$, then by the 3rd equation in (6) we obtain two linear equations in $(\breve{x}, \breve{y})$:

$$\mathbf{A}_2 \begin{pmatrix} \breve{x} \\ \breve{y} \end{pmatrix} = \mathbf{b}_2 \tag{7}$$

where

$$\mathbf{A}_2 \triangleq \begin{pmatrix} \breve{u}p_{21} - \breve{v}p_{11} & \breve{u}p_{22} - \breve{v}p_{12} \\ \breve{u'}p'_{21} - \breve{v'}p'_{11} & \breve{u'}p'_{22} - \breve{v'}p'_{12} \end{pmatrix}$$

$$\mathbf{b}_2 \triangleq \begin{pmatrix} \breve{v}p_{14} - \breve{u}p_{24} \\ \breve{v'}p'_{14} - \breve{u'}p'_{24} \end{pmatrix}$$

And then the point $\breve{\mathbf{X}}$ can be determined linearly with (7).

Our 3D/2D visual metrology algorithm with radial distortion does not need to calibrate the used cameras, and it can be considered as an extension to the triangulation algorithm for perspective cameras [7]. In fact, the 3rd equation in (3) is a back-projecting plane containing a 3D point, and the point can be reconstructed with three back-projecting planes.

3. Experiments

Since our visual metrology with uncalibrated images does not rely on a radial distortion model, here, we generate simulated metrology with a central catadioptric camera. The mirror parameter is $\xi = 0.966$, and the simulated camera intrinsic parameters are:

$$\mathbf{K} = \begin{pmatrix} 700 & 5.0 & 700 \\ 0 & 710 & 750 \\ 0 & 0 & 1 \end{pmatrix} \tag{8}$$

where the principal point $(700, 750)^T$ is known.

3.1 Simulating Experiments

Visual metrology for coplanar points vs. noise level

Nine coplanar points are projected onto two image planes as shown in Figure 1. Five points are known, and the rest four points are to be reconstructed. Gaussian noise with zero mean and standard deviation varying from 0.0 to 1.0 pixel (at the step of 0.2 pixels) is added to the image points and the radial distort center. At each noise level, we perform 100 independent trials, and the reconstructed coordinate with the biggest error is shown in Table 1.

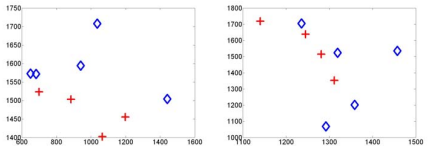

(a) (b)

Figure 1. (a)(b)Two views of 3D points. Two views of coplanar points. Blue squares are known, and red squares are to be reconstructed.

Table 1. Reconstruction of four scene points with two views

Noise level	Reconstruction coordinates			
0.0	(4.00,2.00)	(0.00,4.00)	(2.00,4.00)	(4.00,4.00)
0.2	(3.98,1.99)	(-0.01,4.04)	(2.01,4.03)	(3.98,3.97)
0.4	(4.02,2.05)	(-0.03,4.07)	(1.99,3.90)	(3.93,3.88)
0.6	(4.03,2.06)	(0.06,3.85)	(2.01,3.89)	(3.94,3.90)
0.8	(3.96,1.94)	(-0.09,4.20)	(2.01,3.85)	(4.12,4.16)
1.0	(3.92,1.93)	(-0.08,4.26)	(2.06,4.21)	(4.16,4.16)

Visual metrology for 3D points vs. noise level

Here, nine 3D points are projected onto three image planes as shown in Figure 3. Seven points are known, and the rest two points are to be reconstructed. Similarly, the reconstruction coordinates with the biggest error is shown in Table 2.

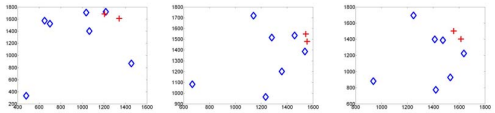

(a) (b) (c)

Figure 2. Three views of 3D points. Blue marks are known, and red marks are to be reconstructed.

The reconstruction results in Table 1 and Table 2 with zero noise are the same as the ground truth, and the reconstructed 2D and 3D points are all close to the ground truth as noise level increases.

3.2 Real Experiments

In the following, the results are tested by real data. Due to the space limitation, only the uncalibrated metrology experiments on a plane are shown here and other experiments having similar results are omitted. Two images of a planar calibration pattern are captured as shown in Figure 3 by moving a NIKON COOLPIX990 with a FC-E8 fisheye lens (under the

Table 2. Reconstruction of two scene points with three views

Noise level	Reconstruction coordinates	
0.0	(2.00, 4.00, 4.00)	(4.00, 4.00, 4.00)
0.2	(2.00, 3.99, 3.99)	(3.99, 3.96, 3.99)
0.4	(2.01, 3.97, 3.96)	(3.99, 3.94, 3.94)
0.6	(2.00, 3.97, 3.97)	(4.00, 3.99, 3.99)
0.8	(1.98, 4.08, 4.09)	(3.99, 3.98, 3.98)
1.0	(2.00, 4.02, 4.03)	(3.99, 3.91, 3.90)

wide-angle mode), the images are of 2048×1536 pixels, and the image point extraction and matching are currently done manually.

Here, we use 10 points to reconstruct the other 15 coplanar points. The metrology results are illustrated in Table 3, and the maximal absolute error is 1.78 cm. The experiment demonstrates that the reconstruction results with uncalibrated images are close the ground truth.

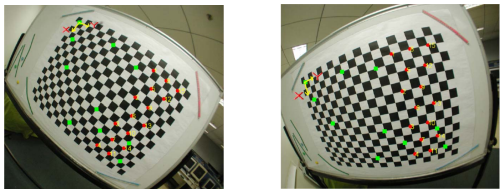

(a) (b)

Figure 3. (a) (b) Two views of coplanar points. Blue marks are known, and red marks are to be reconstructed.

4. Conclusion

The paper presents a novel algorithm for 3D/2D visual metrology of radial distorted images. The main contribution of this paper is that the proposed visual metrology algorithm for radial distorted images does not need specific radial distortion models or calibration, which makes the experiment results more accurate and stable.

In this paper, we concentrate on only the feasibility of metrology with uncalibrated radial distorted images, and we have to point out that the correspondences in this work are manually selected. The further study on automatic image matching and 3D modeling with uncalibrated radial distorted images will be investigated.

Acknowledgement

The authors are grateful to anonymous referees for helpful comments. This work is supported by the National Natural Science Foundation of China(60575019, 60773039), National High Technology R&D Program of China(2006AA01Z116). X. Deng is further supported by National High Technology R&D Program of China (2007AA01Z320).

Table 3. Visual metrology on a plane (RC: Reconstruction coordinate, GT: Ground truth, AE: absolute error)

Points	RC(cm)	GT(cm)	AE (cm)
1	(2.41, 52.81)	(4.00, 52.00)	1.78
2	(19.72, 52.22)	(20.00, 52.00)	0.35
3	(36.05, 52.24)	(36.00, 52.00)	0.24
4	(52.08, 52.00)	(52.00, 52.00)	0.08
5	(11.46, 56.41)	(12.00, 56.00)	0.67
6	(27.84, 56.26)	(28.00, 56.00)	0.31
7	(44.11, 56.11)	(44.00, 56.00)	0.16
8	(2.90, 60.90)	(4.00, 60.00)	1.42
9	(19.71, 60.39)	(20.00, 60.00)	0.49
10	(36.03, 60.24)	(36.00, 60.00)	0.24
11	(51.96, 59.93)	(52.00, 60.00)	0.08
12	(11.46, 64.66)	(12.00, 64.00)	0.85
13	(27.85, 64.34)	(28.00, 64.00)	0.38
14	(44.01, 64.01)	(44.00, 64.00)	0.01
15	(3.01, 69.15)	(4.00, 68.00)	1.51

References

[1] S. Baker and S. Nayer. A theory of single-viewpoint catadioptric image formation. *IJCV*, 35(2):175–196, 1999.

[2] R. Benosman and S. B. Kang. *Panoramic Vision: Sensors, Theory, and Applications*. Springer Verlag, 2001.

[3] A. Criminisi, I. Reid, and A. Zisserman. A plane measuring device. *Image and Vision Computing*, 17(8):625–634, 1999.

[4] A. Criminisi, I. Reid, and A. Zisserman. Single view metrology. *Proc. of ICCV*, pages 434–441, 1999.

[5] F. Duan, F. Wu, and Z. Hu. Pose determination and plane measurement using a trapezium. *Pattern Recognition Letters*, 29(3):223–231, 2008.

[6] A. Fitzgibbon. Simultaneous linear estimation of multiple view geometry and lens distortion. *Proc. of CVPR*, pages 125–132, 2001.

[7] R. Hartley and A. Zisserman. *Multiple View Geometry in Computer Vision*. Cambridge University Press, Cambridge, MA, 2000.

[8] G. Wang, Y. Wu, and Z. Hu. A novel approach for single view based plane metrology. *Proc. of ICPR*, pages 556–559, 2002.

[9] Y. Wu and Z. Hu. Geometric invariants and applications under catadioptric camera model. *Proc. of ICCV*, pages 1547–1554, 2005.

[10] X. Ying and Z. Hu. Can we consider central catadioptric cameras and fisheye cameras within a unified imaging model? *Proc. of ECCV*, pages 442–455, 2004.